2022

# Investigation of Pitching and Plunging Motions on a Tandem Wing Configuration

Riley M. Capiro
*University of Central Florida*

# INVESTIGATION OF PITCHING AND PLUNGING MOTIONS ON A TANDEM WING CONFIGURATION

by

RILEY M. CAPIRO

A thesis submitted in partial fulfillment of the requirements
for the Honors in the Major program in Aerospace Engineering
in the college of Engineering and Computer Science
and in the Burnett Honors College
at the University of Central Florida
Orlando, Florida

Summer Term, 2022

Thesis Chair: Samik Bhattacharya, Ph.D.

## ABSTRACT

From the beginning of the history of flight, inspiration has been drawn from nature. Evolution has spent millions of years optimizing creatures that rely on flight as their means of locomotion. Today, aerial vehicles are very different to those from the time of the Wright brothers. One kind of vehicle that stands to benefit in mimicking nature is the drone, particularly smaller drones. Commonly used today by militaries, industry and civilians, drones are increasingly affordable while also decreasing in size thanks to advancements in electronics and manufacturing methods. The purpose of this thesis is to investigate how pitching and rolling motions interact with a tandem wing.

The effect of a tandem wing is mostly apparent in the hind wing, as the fore wing moves through the fluid it energizes the flow and creates a wake region. The energy put into the fluid is otherwise lost unless captured by the hind wing. The damselfly was essential inspiration in the development of this experiment, current research shows that higher levels of efficiency can be achieved by mimicking the creature's anatomy. A pitching and plunging motion by the hindwing seeks to recreate the flapping motion used by the damselfly. Particle Image Velocimetry (PIV) was carried out on both wings to visualize the flow and develop an idea of the flow physics at work.

Early results show the combined pitching and plunging motion are an effective means of vortex generation. These vortices create a pressure gradient across the hindwing, contributing to lift generation. This is particularly of interest in the take-off phase of flight. The flapping motion has the dual purpose of producing lift and thrust, this is seen as it shifts between downstroke and upstroke of the plunging cycle.

# Table of Contents

# LIST OF FIGURES

# LIST OF TABLES

# LIST OF ACRONYMS

| | |
|---|---|
| MAV | Micro air vehicle |
| PIV | Particle image velocimetry |
| LEV | Leading-edge vortex |
| TEV | Trailing-edge vortex |
| PLA | Poly-lactic acid |
| FW | Forewing |
| HW | Hindwing |
| OEM | Original Equipment Manufacturer |

# CHAPTER ONE: INTRODUCTION

Biomimicry, the use of biological entities as inspiration for design, has been present in aviation from the very beginning. Early airfoils used highly cambered surfaces designed to imitate birds, and concepts dating back to the time of Leonardo da Vinci incorporated wings that could flap as means of generating lift. Today, the world of aviation is very different from what it was, but the use of biomimicry is still very relevant. A significant challenge researcher are faced with now is reducing the size of aerial vehicles for civilian and military applications. Solving this challenge would allow for the application of Micro Air Vehicles (MAVs) to urban scenarios, in life threatening situations MAVs can provide rescue teams with critical information (Ng & Leng, 2002).

Traditional aircraft design can not be applied to MAVs, these vehicles operate in low Reynold's number regimes where the governing physics operate under different principles. Lift generation is a considerable issue affected by the complex flow phenomena present in the boundary layer. These small vehicles must contend with separation, transition, and reattachment of their boundary layers within very small distances, making them sensitive to interference (Pines & Bohorquez, 2006).

Many current vehicles manage this through the use of rotary-wing designs, similar systems are present in marine vehicles as a means of propulsion. While they have shown results, these systems fail to recapture energy expended into the flow (Lehmann, 2008) leading to lower efficiency. A more efficient design would enable lighter battery packs and a smaller cross-section allowing for improvement in MAV performance. The unsteady flapping motion of insects and birds may provide the necessary solution for lift generation and

propulsion. These creatures maintain high levels of agility through the manipulation of the unsteady flow field. They must navigate a host of situations from take-off to landing and rely on flight for much more than transportation, it is their means of finding food and evading predators, flight is essential to their survival.

Past research has shown the benefits of a tandem wing configuration and has begun to incorporate pitching and plunging motion, but focus has been placed on power consumption in relation to lift and thrust generation (Lehmann, 2008) (Felli, 2020) (Broering & Lian, 2012). This thesis reviews previous works that have expanded our understanding of tandem flapping wings and seeks to visualize the flow in order to better describe the fluid mechanics at work. The wake region and trailing-edge vortex (TEV) of the forewing are particularly of interest as it affects the leading-edge vortex (LEV) of the hindwing and results in changes in aerodynamics force production and efficiencies.

To achieve this, a custom-built experimental setup was used to pitch and plunge a pair of rigid insect-like wings through a water tank over a set of conditions. Particle Image Velocimetry (PIV) measurements were carried out at different stages of the plunging cycle to observe the wing wake interaction and boundary layer of the heaving hindwing. Special attention was placed on the leading-edge vortex of this wing.

# CHAPTER TWO: LITERATURE REVIEW

The flight of insects and birds, and the general study of flight, has been under investigation for many of the last centuries. Kites dating back to 400 B.C. have been found in China for use in ceremonies and as instruments for measuring weather conditions. The first real studies of flight were made by Leonardo da Vinci who illustrated his theories on avian and mechanical flight (Bellis, 2018).

Formal experimental research saw a huge leap with the development of the Reynolds number concept. Named after Osborne Reynolds, the concept was based on the ratio of inertial to viscous forces in a fluid and its relation to the flow regime (Rott, 1990). In fluid mechanics, nondimensionalization is common and the Reynolds number is no exception, it is valued for its ability to characterize a flow regime. It allows the reader to develop some idea of where the flow lies on the spectrum between laminar and turbulent flow, where lower values typically indicate laminar and higher values suggest turbulent flow. Shown below in Equation 1 is the relation.

$$Re = \frac{\rho U_\infty L_c}{\mu} = \frac{U_\infty L_c}{\nu} \tag{1}$$

The Reynolds number equation as previously mentioned is a ratio of inertial to viscous forces. In the numerator are the inertial terms, $\rho$ represents density of the fluid, $U_\infty$ is the free stream velocity, and $L_c$ is the characteristic length which represents the chord of the wing. In the denominator is the viscous term $\mu$, representing the viscosity of the fluid.

The density and viscosity term may also be represented by the kinematic viscosity term ν, where $\frac{\rho}{\mu} = \frac{1}{\nu}$.

Soon after the development of the Reynolds number concept was a breakthrough in the modeling of lift of an airfoil. A relationship between lift and circulation was established by mathematician M. Wilhelm Kutta and physicist Nikolai Joukowski. Now known as the Kutta-Joukowski theorem, it states that the lift per unit span of an airfoil is proportional to the circulation around the airfoil (Schmitz, 2014). Shown below in Equation 2 is the theorem.

$$L' = \rho U_\infty \Gamma \tag{2}$$

The lift per unit span is denoted by $L'$ and is the product of; $\rho$ the density of the fluid, $U_\infty$ the free stream velocity of the fluid, and $\Gamma$ the circulation around the airfoil. This relationship may be applied for inviscid and irrotational flow conditions. Its applicability lies mostly in high-Reynolds-number attached flow and is an essential component in modeling stall. Stall is a condition of winged flight in which there is a sudden drop in lift when the lifting surface is pitched beyond the critical angle of attack. This effect particularly concerns MAVs, their lower operating speeds affects their ability to generate lift (Pines, Bohorquez, 2006). Due to this limitation many MAVs have implemented a rotary-wing design, this approach allows for effective lift generation. However, these systems generally lack the agility and fail to recapture energy expended into the flow (Lehmann, 2008).

An alternative approach is to employ flapping wings as a means of lift generation and propulsion. These systems have been shown to be effective at the size scale of an MAV (Deng, Wang & Liu, 2019). This is a logical conclusion as the birds and insects that have adopted this

system operate at similar length scales with Reynolds numbers in the same order of magnitude. Insects such as dragonflies and damselfly employ flapping motion with a tandem wing to achieve flight. They are some of the fastest and most maneuverable flying insects, they have evolved to overcome the viscous effects that restrict lift and thrust generation (Broering & Lian, 2012). It is through the control of unsteady flow that they are able to overcome these viscous effects (Yu & Guan, 2014).

A significant trait of the tandem wing configuration is that the hindwing interacts with the wake of the forewing. This arrangement coupled with flapping motion introduces various mechanisms for generating lift, including wake capture and leading-edge vortex development (Rival, Hass & Tropea, 2011). To characterize and analyze the unsteady flow resulting from flapping motion a relation is needed. Walter Birnbaum, a German physicist, would develop a relationship between two characteristic speeds while studying flow over an oscillating airfoil (Birnbaum 1954). This nondimensionalized parameter, known as the reduced frequency, is shown below in Equation 3.

$$k = \frac{\omega b}{V} \mid \omega = 2\Pi f \mid b = \frac{C}{2} \mid \mathrm{V} = U_\infty \mid \mathrm{k} = \frac{\Pi f C}{U_\infty} \tag{3}$$

Here k represents the reduced frequency, $\omega$ is the circular frequency of flapping, b is the mid chord of the wing, where C is the full chord, and $U_\infty$is the free stream velocity. This parameter while extremely useful is best applied to two-dimensional scenarios as the tip of the wing is not considered.

With a relationship established for the flapping motion, one is needed to relate plunging to the forward motion of the object. A useful parameter for this is the Strouhal number, shown below in Equation 4.

$$St = \frac{fh}{U_\infty} \tag{4}$$

Named after Vincenc Strouhal, the relation relates; f the flapping frequency, h the heaving amplitude and $U_\infty$ the free stream velocity (Taylor, Nudds, & Thomas, 2003). Experiments by Taylor on flying and swimming creatures revealed optimal propulsive efficiency to lie within the range 0.2 < St < 0.4 due to improved LEV formation. Where the Strouhal number fails to evaluate flapping motion is in cases of varied angle of attack. A study by Yeon Sik Baik found the effective angle of attack $\alpha_{eff}$ and the reduced frequency better determine the evolution of the flow (Baik, Bernal, Granlund, & Ol, 2012). Shown below in Equation 5 is the definition of the effective angle of attack.

$$\alpha_{eff} = \alpha_0 + \theta(t) + tan^{-1}\left(-\frac{1}{U_\infty}\left(\frac{dh}{dt}\right)\right) \tag{5}$$

Here $\alpha_0$ is the mean pitching amplitude, $\theta(t)$ is the geometric pitch angle as a function of time and $U_\infty$ is the free stream velocity. The heaving amplitude is h, when differentiated over time in the $\frac{dh}{dt}$ term it becomes the heaving velocity (Baik, Bernal, Granlund, & Ol, 2012).. This definition is best applied when the flow remains attached at small effective angles of attack, when considering detached flow and high effective angles of attack another definition is needed. Work by Gursul and Cleaver has shown the reduced frequency to be more

significant in the detached flow condition (Gursul & Cleaver, 2018). Shown below in Equation 6 is their definition.

$$\alpha_{eff} = \alpha + tan^{-1}\left(\frac{U_{pl}}{U_{\infty}}\right) \tag{6}$$

Here $\alpha$ is the geometric angle of attack, $U_{pl}$ is the heaving velocity and $U_{\infty}$ is the free stream velocity. The need to understand the effective angle of attack in detached flow conditions is essential to this area of research as it relates to the low-speed viscous effects previously mentioned. Traditional aircraft design can not be applied in this area and the physics of a higher Reynolds number regime are not always applicable.

The ability to develop better control of a tandem flapping wing is the inspiration behind this thesis. For a better understanding, the flapping motion is studied through pitching and plunging of two insect like wings. This research will focus particularly on vortex formation and the behavior of the hindwing in the wake of the forewing. Flow visualization with PIV will reveal these vortices and give insight into the effects of a tandem wing configuration.

# CHAPTER THREE: METHODOLOGY

Experiments for this research were carried out on a custom-built setup that allowed for PIV measurement. These measurements were taken repeatedly to confidently establish the behavior of the setup. The working fluid for this experiment is water contained within a tank commonly used by aquarium hobbyists. The main goal of the experiment was to visualize the flow surrounding a pitching and plunging tandem wing. The processed PIV results allow for a better interpretation of the flow physics at work. All experimental work was conducted at the Experimental Fluid Mechanics Laboratory located on the University of Central Florida (UCF) campus.

## Wing Description

A significant inspiration for this thesis was the damselfly, this insect is extremely agile and has the potential to benefit MAV development. The wings used for this experiment were cut from thin acrylic sheets, the design used was made in the computer-aided design software (CAD) Solidworks. Their design was intended to imitate the profile of a damselfly wing as realistically as possible. A diagram of the forewing (FW) and hindwing (HW) is presented below in Figures 1 and 2 respectively. A table containing the specific design variables of each wing is presented in Table 1 below.

Table 1: Wing Design Variables

| Parameter | Symbol | FW Value | HW Value |
|---|---|---|---|
| Chord | C | 2.6cm | 3.2cm |
| Span | S | 9.95cm | 10cm |
| Thickness | T | 5.0mm | 5.0mm |

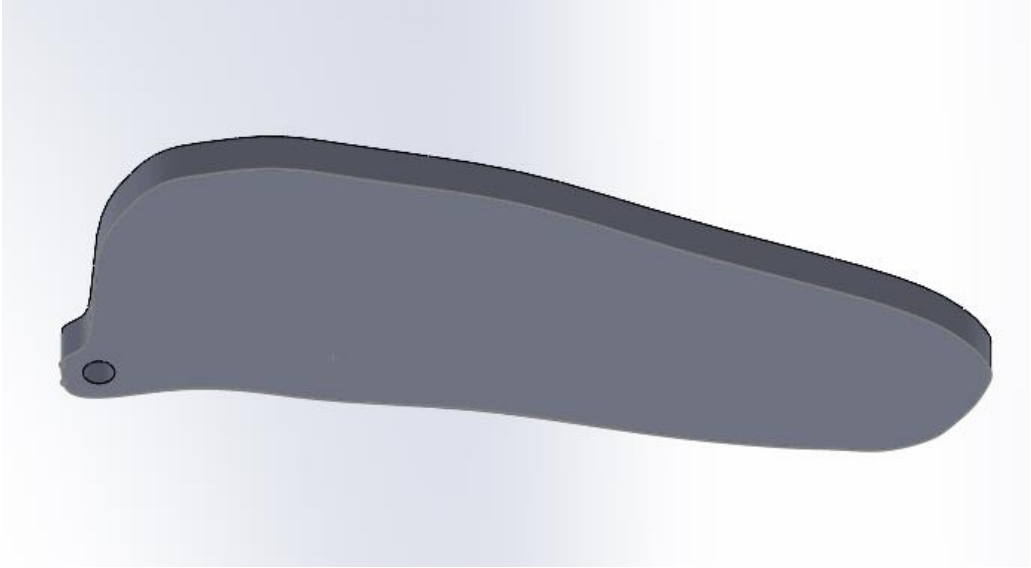

Figure 1: Forewing

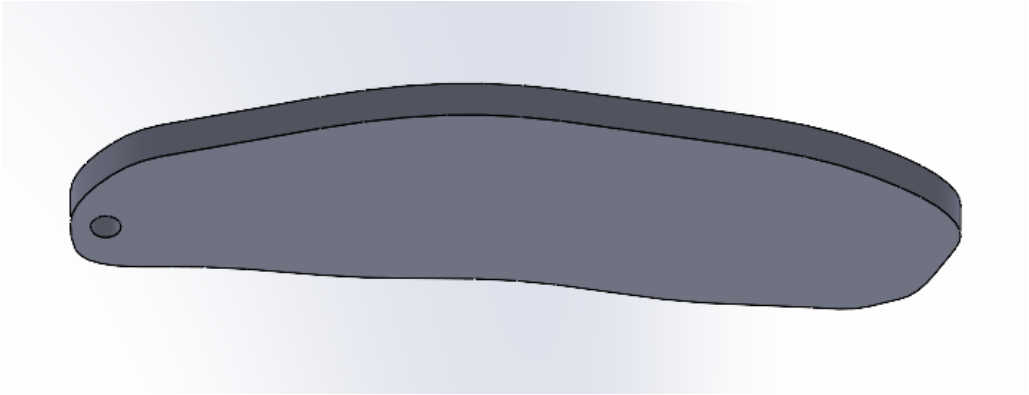

Figure 2: Hindwing

The wings were manufactured using the resources at the UCF Innovation Lab. There the CAD designs for the wings were fed to an automated laser cutter that cut the wings from a larger sheet of acrylic. A small hole was added on each wing to allow for supporting hardware.

## Pitching and Plunging Mechanism

The pitching and plunging motions needed to simulate the motions of a damselfly wing were created through the use of rotational and linear electronic motors. These motions

were carried out by the hindwing while the forewing remained in a relatively static position. Both wings were mounted to a traverse system capable of accelerating them to the free stream velocity. Shown below in Figure 3 is the tandem wing configuration mounted on the traverse system.

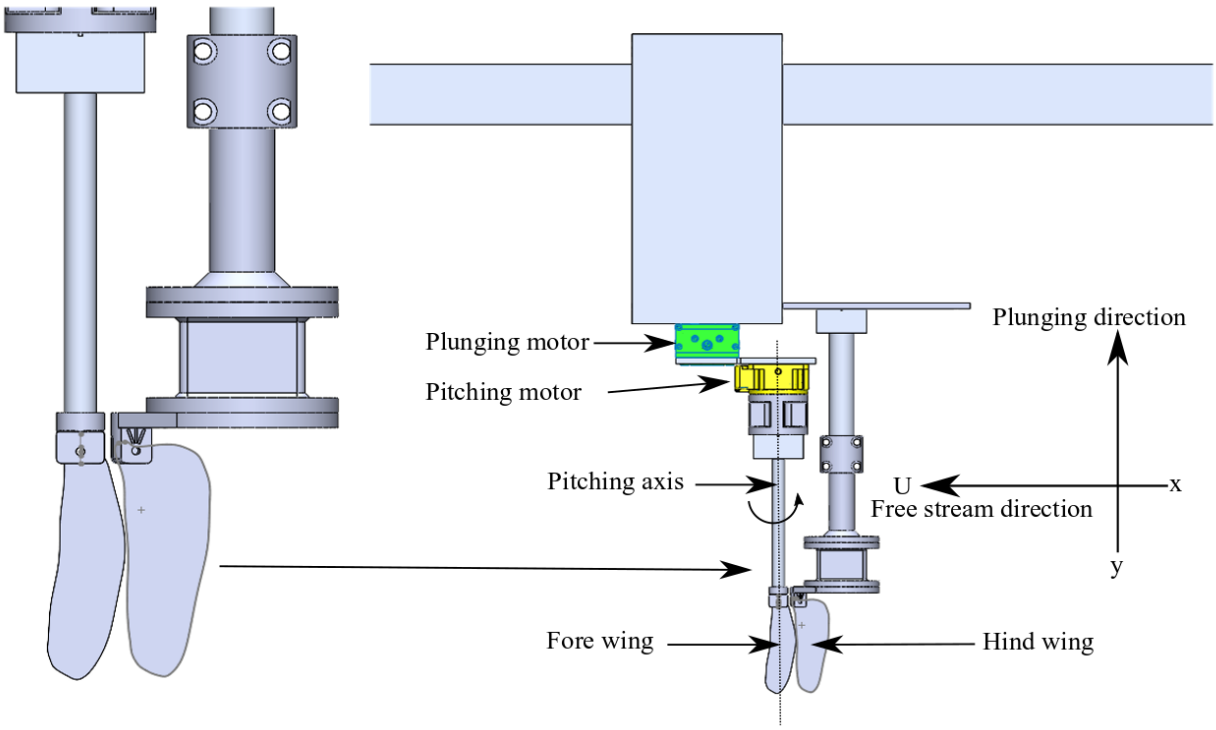


Figure 3: Pitching and Plunging Mechanism

The plunging motor shown in the figure above is a Zaber LSQ150B-T3, the rotary stage motor, Zaber RSW60A-T3, is connected via an aluminum plate. Linking these two motors allows for a more complex pitching and plunging motion combination which more closely mimics the flapping of the damselfly. The rotary motor then connects to a poly-lactic acid (PLA) plastic adapter which supports an aluminum block and rod that hold the hindwing. The forewing uses a much simpler support structure, all parts were 3D printed

from PLA and secure the wing firmly in place. A geometric angle of attack of $\alpha$ = 0° was maintained by this wing throughout all measurements. The pitching motion is a rotation about the supporting aluminum rod which aligns with the mid chord of the hindwing. The plunging motion maintains a constant distance between the two wings throughout the whole cycle. The linking of the linear and rotary motor allows for the angle of attack to be dynamic, the angle may change as the wing plunges.

A Zaber X-MCB2 multi-axis controller using Zaber Console software was programmed to synchronize motor control with other experimental equipment. The plunging motion programmed through the Zaber Console used amplitude and frequency, Equation 7 below shows this analytically.

$$h = h_0 \sin\left(2\Pi f t + \frac{\Pi}{2}\right) \tag{7}$$

Here $h_0$ is the heaving amplitude in meters, f is the frequency in cycles per second and t is the time in seconds. The $\Pi/2$ term is added as an offset, so the heaving motion begins from its furthest point. The previously mentioned traverse system accelerates the forewing and hindwing to the freestream velocity of $U_\infty$= 0.05 m/s. This is the velocity used throughout all measurements. The kinematic viscosity of the water in the tank is assumed to be $\nu$ = 1 x $10^{-6}$ $m^2/s$. The combination of these variables returns a constant chord-based Reynolds number of Re = 1300, when using the forewing chord. The traverse system is controlled through software provided by the original equipment manufacturer (OEM).

Dynamic pitching is governed by a relation similar to that used for plunging. In all measurements the initial angle of attack is $\alpha_0$ = 5˚. In half the period the wing pitches to its maximum angle of attack $\alpha_{max}$ = 45˚. Equation 8 shows this below.

$$\alpha = 40\sin(ft) + \alpha_0 \tag{8}$$

Here $\alpha$ is the geometric angle of attack of the hindwing, f is the frequency in Hz, and $\alpha_0$ is the initial angle of attack added as an offset. For these experiments the hindwing was set to oscillate between an initial and maximum angle of attack of, 5˚ and 45˚ respectively. The $\alpha_0$ term is added as an offset so the wing begins at 5˚ when time is 0. The coefficient of the sin term is 40, this results in $\alpha_{max}$ = 45˚ at the midpoint of the period.

## Experimental Setup

The tank used for these experiments is composed of transparent glass and measures 36 x 18 x 16 in (length x width x height) with 0.1875-in-thick walls. The traverse system previously mentioned is a FUYU FSL120 powered by a Panasonic MINAS A6 servo motor controlled by OEM software from FUYU. A manual trigger switch is used to initiate linear translation. Figure 4 below shows the setup.

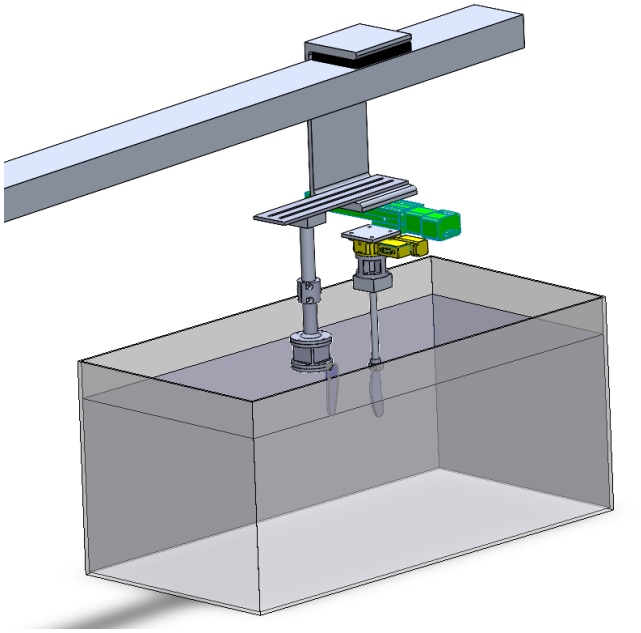

Figure 4: Model of Experimental Setup

## Measurement Techniques

### Particle Image Velocimetry (PIV)

PIV experiments are carried out by generating a laser plane perpendicular to the chord line of the wing to illuminate particles suspended in the water tank. The illuminated particles are neutrally buoyant and move in the same manner as the flow field developing in the tank. A highspeed camera is positioned perpendicular to the laser plane and is used to record the illuminated particles as the wing passes through. A schematic of the PIV setup used in this research is shown below in Figure 5 with the laser shown in blue and the laser plane shown in green.

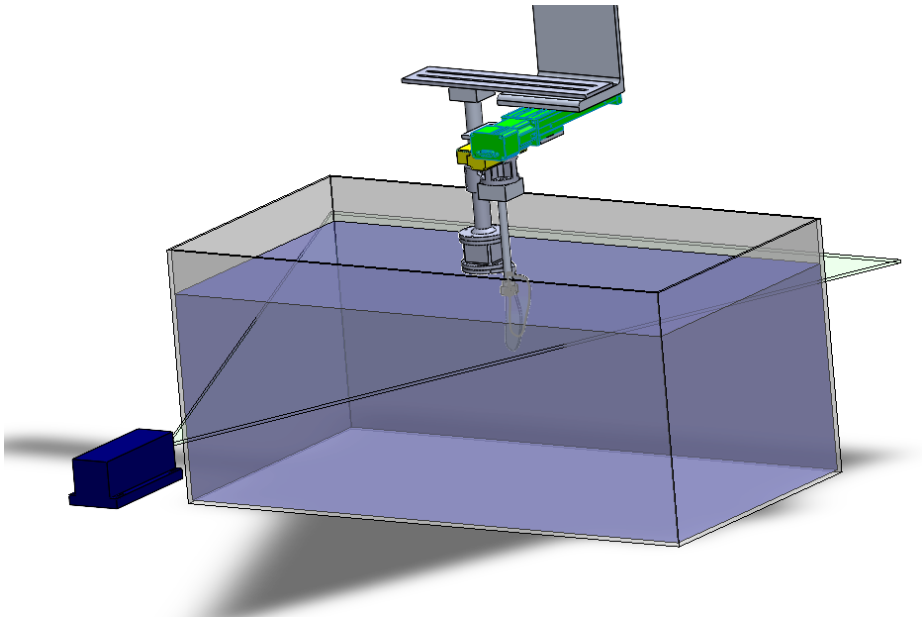

Figure 5: Model of PIV setup

The laser plane was generated using a Changchun New Industries (CNI) MGL-F-532 diode-pumped solid-state laser. The laser beam is passed through a Thorlabs cylindrical lens that flattens and spreads out the laser to cast a plane. The laser is mounted on an external custom-built laser rig that accurately casts the plane parallel to the surface of the water, for accurate results the plane must remain level. PIV measurements were taken at 50% span as measured from the root. All measurements recorded one heaving cycle, at a plunging frequency of 0.5 Hz this results in a period of 2 seconds.

For improved illumination, Conduct-O-Fil silver coated-glass spheres provided particle seeding. PIV recordings were carried out using a PCO 12000HS high speed camera recording at a frequency of 200 Hz and an exposure time of 5 ms. The camera is controlled using PCO Camware, its OEM software. The recording sequence is initiated through the same manually activated trigger switch previously mentioned, a delay is included so the period of

acceleration is not recorded. After the delay, an Arduino controller relays a signal to the PCO Camware software to begin the recording sequence.

## Parameter Space

Taking the size of the tank into consideration a small test section length was preferred. Additionally, the setup aims to provide a nondimensionalized reduced frequency of k = 1.0. The test length was selected to be 100 mm, at a freestream velocity of $U_\infty$ = 0.05 m/s this yields a period of T = 2 s. The frequency needed to complete a heaving cycle in 2 seconds is $f$ = 0.5 Hz. Many of the design parameters are nondimensionalized for analytical purposes. These nondimensional parameters are presented below in Table 2.

Table 2: Nondimensional Parameters

| Parameter | Definition |
|---|---|
| Reynold's number | $\mathrm{Re} = \frac{UC}{v}$ |
| Reduced frequency | $k = \frac{\pi f C}{U_\infty}$ |
| Nondimensional heaving amplitude | $h^* = \frac{h}{C}$ |
| Strouhal number | $\mathrm{St} = \frac{fh}{U_\infty}$ |

The reduced frequency of k = 1.0 is of interest to this thesis as it lies in the unsteady flow regime. A flow is considered to be in the unsteady regime for reduced frequency values of k > 0.2 (Leishman, 2016). A Reynolds number of 1300 was selected since it is a good representation of the flow regime in which the damselfly and similar insects normally operate (Lehmann 2008). Using the heaving amplitude, 3.75 cm, the Strouhal number is

found to be 0.375, this reflects the Strouhal number of natural flyers and swimmers. The range of these creatures is typically $0.2 < St < 0.4$ (Taylor, Nudds, & Thomas, 2003).

## Data Processing

### PIV Data

The high-speed camera used for PIV outputs a set of frames for each testing segment. Each set of frames contains more than what is needed for analysis. The sets of frames are trimmed to show a 2-second segment of the heaving cycle via MATLAB code. Frame pairs in intervals of 10 are selected, through MATLAB, for PIV processing. The selected frames are imported into PIVlab, a MATLAB extension that functions as a PIV processing software. PIVlab can take the frame pairs and use them to calculate the velocity vectors and vorticity of the flow field for each frame.

# CHAPTER FOUR: RESULTS

The dynamic pitching and sinusoidal plunging motions of a tandem wing were investigated to develop an understanding of the flapping motions used by insects like the damselfly. These motions are explored throughout the results section using the PIV data collected. The PIV measurements allow for study of the fluid-structure interactions and flow field development about the wings.

## Effects of Dynamic Pitching and Sinusoidal Plunging

The combination pitching and plunging motion is the main interest of this study, since its effects are notable in flapping motion. As previously mentioned, the hindwing begins its motion offset by half the plunging amplitude ($h_0/2$), at an angle of attack of $\alpha_0$ = 5°. Figure 6 below shows the initial position of both wings as viewed from above.

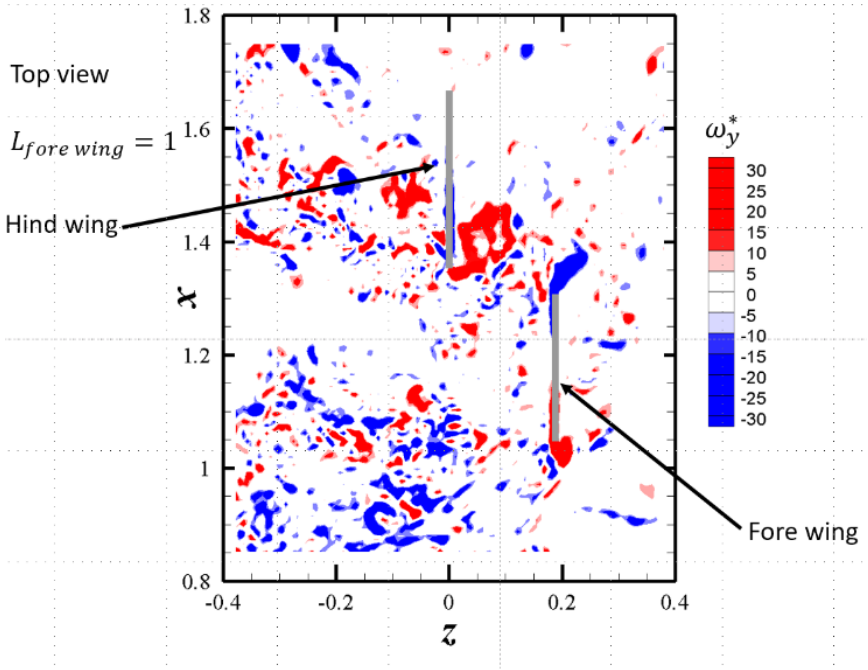


Figure 6: Tandem wing initial positions

The motions occurring from time t = 0 s to t = 1 s are considered the downstroke. In this period of time the angle of attack progresses from 5˚ to 45˚, the plunging motion reaches half the plunging amplitude as measured from the opposing side of the forewing. The restoring motion to the initial angle of attack and plunging position is considered the upstroke, this takes place from time t = 1 s to t = 2 s. Figures 7 and 8 show the initial and mid-cycle positions of the forewing and hindwing.

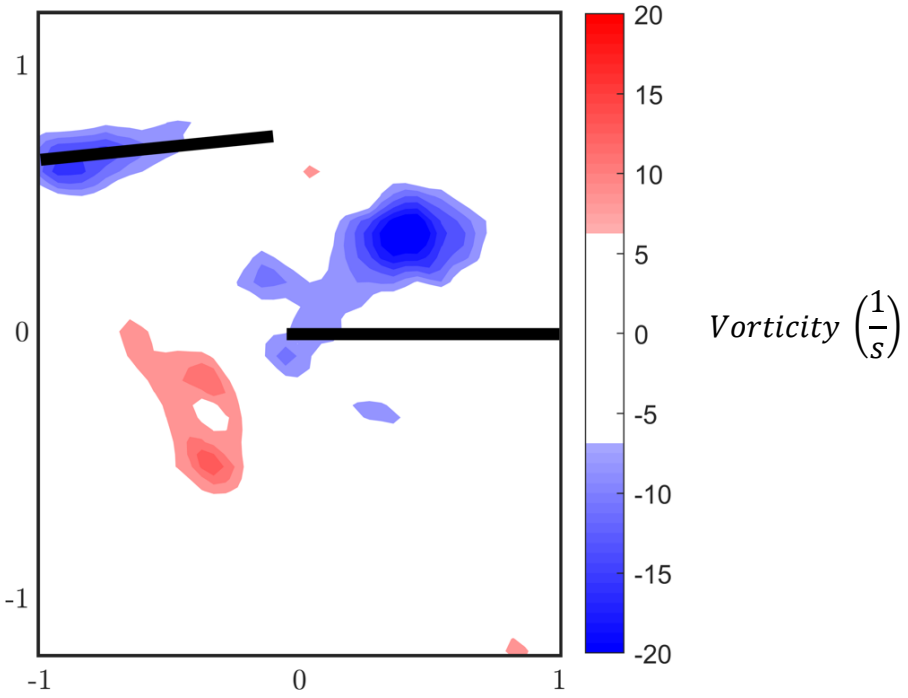


Figure 7: Wing position at t = 0s (Top View)

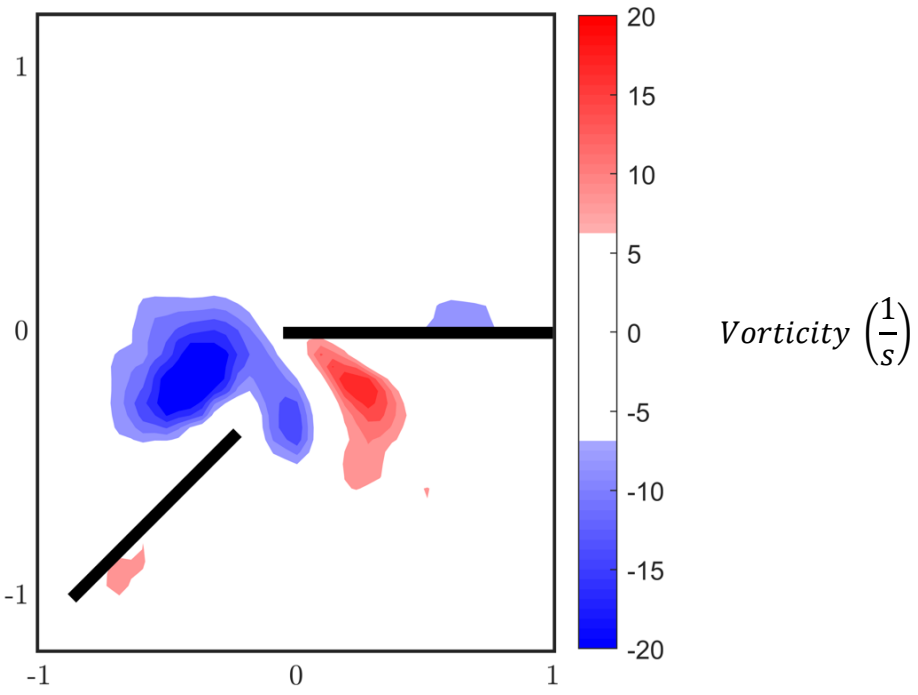


Figure 8: Wing positions at t = 1s (Top View)

In Figures 7 and 8, the vorticity of the flow is shown using a color gradient where red indicates positive vorticity and blue indicates negative vorticity. Positive vorticity suggests counterclockwise motion, while negative vorticity rotates clockwise. A comparison between frames taken during the upstroke and downstroke show the formation of a LEV and TEV on the hindwing. As can be seen in Figure 8, the downstroke motion forms a region of negative vorticity. As the hindwing returns to its original position this vortex curls about the leading edge and is left in the wake of the hindwing. Figure 9 below shows the upstroke motion of the hindwing at time t = 1.5 s forming a region of positive vorticity.

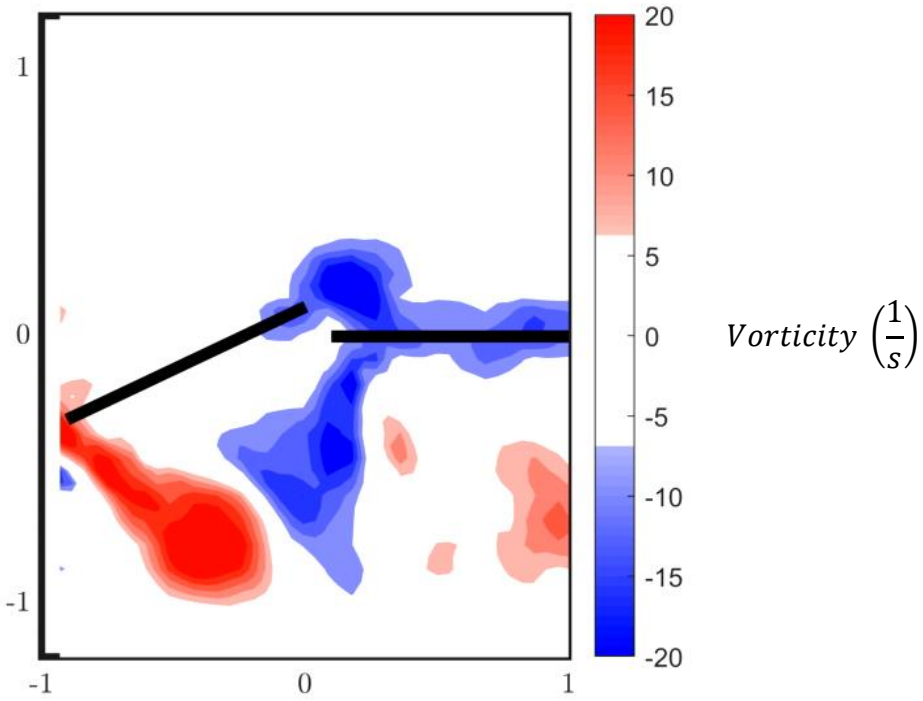


Figure 9: Wing positions at t = 1.5s (Top View)

Figure 9 reveals the formation of a vortex on the hindwing as it returns to its initial position. The heaving of the wing is not the only factor to consider in the formation of these vortices. The maximum angle of attack of $\alpha_{max}$ = 45° is achieved 0.5 s before, at the point between the downstroke and the upstroke. The vortex that forms on the suction surface as the wing approaches $\alpha_{max}$, is typical of lifting surfaces and can be seen in dynamic stall experiments. What is atypical is the formation of a TEV, because of the heaving motion this vortex forms opposite the suction surface, as observed from the downstroke.

It is essential to note that the hindwing does not have fixed pressure and suction surfaces, these alternate throughout the heaving motion. Figure 10 below shows an entire

cycle using nondimensionalized time $t^* = \left(\frac{t}{T}\right)$, the cycle takes place between $t^* = 8.0$ and $t^* = 9.0$. A time step of 0.25 s separates each image.

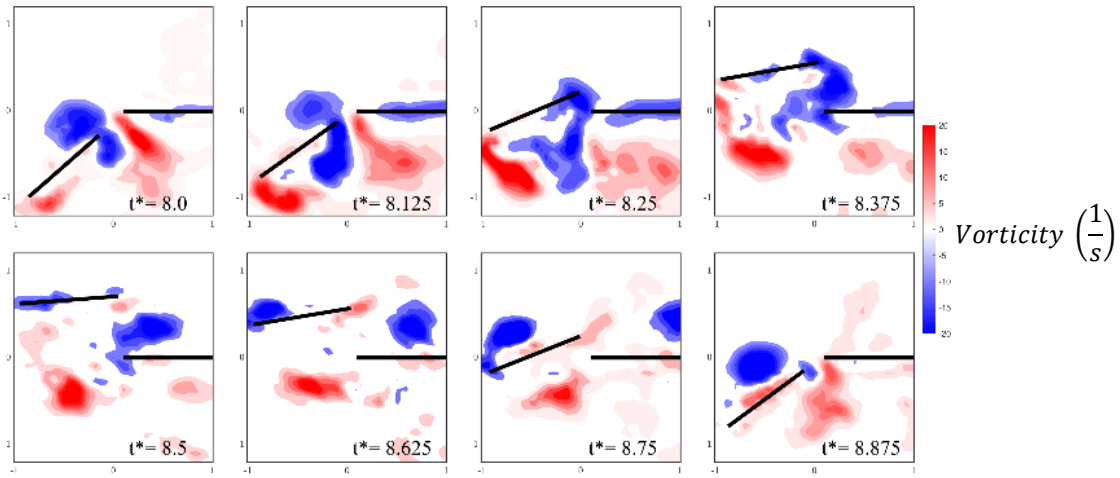


Figure 10: Pitching and plunging cycle over nondimensionalized time

Closer observation of the images in Figure 10 reveal that the vortex formed during the downstroke begins its growth from the trailing edge. As the wing shifts plunging directions this vortex is shed about the leading edge. At time $t^* = 8.75$ the blue region shows a pocket of negative vorticity forming from the trailing edge, this region separates and migrates along the chord towards the leading edge. At time $t^* = 8.0$, which may effectively be treated as taking place 0.5 s after $t^* = 8.75$, the vortex has begun separation about the leading edge. The flow field develops similarly in each cycle, so the images shown can be studied as continuous repeating behavior.

At time $t^* = 8.25$ the interaction of the shedding LEV and newly formed TEV is captured. The LEV and TEV interaction is significant as it forms the wake region of the hindwing during the upstroke. These vortices may improve circulation about the wing and

reduce the pressure on the suction surface. These factors would result in more effective lift generation and may explain why insects like the damselfly have adopted this behavior. Additionally, the plunging velocity is greatest as the mid-chord of the hindwing passes through the chord line of the forewing. A high plunging velocity increases the effective angle of attack and shear layer velocity. Under these conditions vortices can rapidly form and shed into the wake of the hindwing, further contributing to lift generation.

## Effects of a Secondary Wing

In nature, small insects have evolved to use a tandem wing configuration. Many benefits have been observed from this feature, but it is not found in larger creatures. This is an indication that its benefits may only be employed in the flow regime occupied by these small insects. PIV data suggests the forewing assists the hindwing in vortex shedding. This can be seen in Figure 11 below.

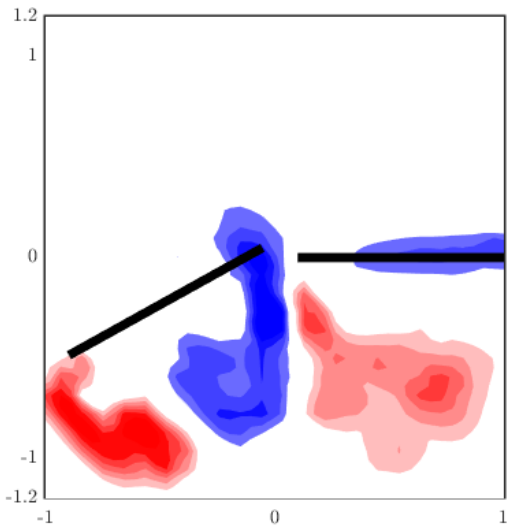


Figure 11: LEV and TEV interaction

Figure 11 is an image captured just before t = 1.5 s, it shows vortices being shed from the leading and trailing edge of the hindwing into the wake. As the hindwing moves through the upstroke the LEV collides with the forewing, this assists its shedding into the wake. Further wing spacing would not have the same effect, so this provides some explanation as to why damselflies have developed tightly packed wings.

Because the hindwing operates in the wake of the forewing the flow is energized and may allow for improved vortex formation. Figure 12 shows the relative motion of the wings.

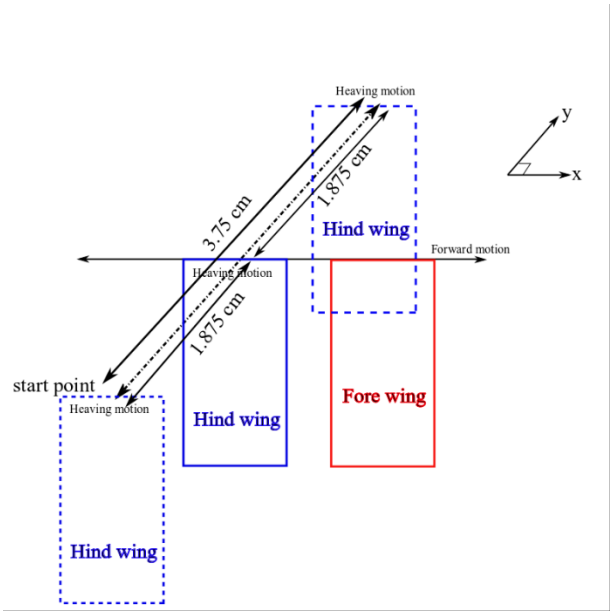


Figure 12: Tandem wing motion

From Figure 12 it is clear the hind wing enters the wake region of the forewing at the midpoint of the plunging motion. As previously discussed, the velocity of the hindwing is greatest at this point. A higher plunging velocity increases shear layer velocity which improves vortex formation and shedding. This coupled with the wake of the forewing suggest amenable conditions for vortices.

# CHAPTER FIVE: CONCLUSION

Two damselfly-like wings arranged in tandem, with a flapping motion of the hindwing was investigated. The effect of pitching, plunging, and a secondary wing on the flow field was evaluated using PIV measurements. These measurements recorded a 2 second period of dynamic pitching and heaving in the wake of the forewing.

Dynamic pitching largely dictated the region of vortex formation and the direction in which these vortices were shed. During the upstroke motion, dynamic pitching led to most vorticity forming on the suction surface of the hindwing. This tendency coupled with the plunging motion allows for propulsion from the pressure surface and effective lift generation from the suction surface. This supports the choice of a St = 0.375 Strouhal number as it falls within the range of $0.2 < St < 0.4$, which is common for natural flyers like the damselfly (Taylor, Nudds, & Thomas, 2003). All measurements utilized a reduced frequency of k = 1.0, an unsteady flow regime (Leishman, 2016). The flow field shows promise in lift generation and propulsion so there is reason to believe the damselfly relies on unsteady flow for its locomotion.

The pitching and plunging motions benefit from their combined use. As previously shown in Equation 5, the effective angle of attack increases with plunging velocity. This suggests the heaving motion improves lift generation by exaggerating the pitching motion. At the point of maximum heaving velocity, the hindwing passes through the wake of the forewing, this allows the hindwing to more effectively shed the LEV. The energized flow in the wake may also contribute to vortex growth which affects lift generation.

Follow up experiments are suggested to better explore the flow field that forms as a result of a tandem flapping wing. Due to limitations of the setup the forewing could not

perform dynamic motions. Modifications that would allow for dynamic pitching and plunging of the forewing would better replicate the real motions of the damselfly. PIV measurements were limited by laser positioning, several measurements along the span of the wings would allow for construction of a 3D model.

Force sensor data would yield values for lift and drag and would complement the PIV data. These values could be used to calculate circulation in the flow field using the Kutta-Joukowski theorem. Many studies have placed an emphasis on energy usage and quantification of propulsive efficiency, the force sensor would allow for similar study. Lastly, it is suggested to include analysis of Strouhal number and reduced frequency, these parameters consider heaving amplitude, freestream velocity and flapping frequency. They are valuable to any study of flapping motion.

## REFERENCES


Baik, Y. S., Bernal, L. P., Granlund, K., & Ol, M. V. (2012). Unsteady force generation and vortex dynamics of pitching and plunging airfoils. Journal of Fluid Mechanics, 709, 37- 68. doi:10.1017/jfm.2012.318

Bellis, M. (2018, September 24). *The early history of Flight*. ThoughtCo. Retrieved July 23, 2022, from https://www.thoughtco.com/early-history-of-flight-4072777

Birnbaum, W. (1954). THE PLANE PROBLEM OF THE FLAPPING WING. *National Advisory Committee for Aeronautics*.

Broering, T. M., & Lian, Y.-S. (2012). The effect of phase angle and wing spacing on tandem flapping wings. *Acta Mechanica Sinica*, *28*(6), 1557–1571. https://doi.org/10.1007/s10409-012-0210-8

Deng, S., Wang, J., & Liu, H. (2019). Experimental study of a bio-inspired flapping wing MAV by means of force and Piv Measurements. *Aerospace Science and Technology*, *94*, 105382. https://doi.org/10.1016/j.ast.2019.105382

Felli, M. (2020). Underlying mechanisms of propeller wake interaction with a wing. *Journal of Fluid Mechanics*, *908*. https://doi.org/10.1017/jfm.2020.792

Gursul, I., & Cleaver, D. (2018). Plunging Oscillation of Airfoils and Wings: Progress, Opportunities, and Challenges. AIAA Journal, 57(9), 3648-3665. doi:10.2514/1.J056655

Lehmann, F.-O. (2008). Wing–wake interaction reduces power consumption in insect tandem wings. *Experiments in Fluids*, *46*(5), 765–775. https://doi.org/10.1007/s00348-008-0595-0

Leishman, J. G. (2016). Principles of Helicopter Aerodynamics. Cambridge, United Kingdom: Cambridge University Press.

Ng, T. T. H., & Leng, G. S. B. (2002). Application of genetic algorithms to conceptual design of a micro-air vehicle. *Engineering Applications of Artificial Intelligence*, *15*(5), 439–445. https://doi.org/10.1016/s0952-1976(02)00072-6

Pines, D. J., & Bohorquez, F. (2006). Challenges facing future micro-air-vehicle development. *Journal of Aircraft*, *43*(2), 290–305. https://doi.org/10.2514/1.4922

Rival, D., Hass, G., & Tropea, C. (2011). Recovery of energy from leading- and trailing-edge vortices in tandem-airfoil configurations. *Journal of Aircraft*, *48*(1), 203–211. https://doi.org/10.2514/1.c031062

Rott, N. (1990). Note on the history of the reynolds number. *Annual Review of Fluid Mechanics*, *22*(1), 1–12. https://doi.org/10.1146/annurev.fl.22.010190.000245

Schmitz, S. (2014). Finite domain viscous correction to the Kutta–Joukowski theorem in incompressible flow. *AIAA Journal*, *52*(9), 2079–2083. https://doi.org/10.2514/1.j053114

Taylor, G. K., Nudds, R. L., & Thomas, A. L. (2003). Flying and swimming animals cruise at a Strouhal number tuned for high power efficiency. Nature, 425, 707-711. doi:https://doi.org/10.1038/nature02000

Yu, Y.-l., & Guan, Z.-w. (2014). Aerodynamic mechanism of forces generated by twisting model-wing in bat flapping flight. Applied Mathematics and Mechanics, 35(12), 1607-1618. doi:10.1007/s10483-014-1882-6